Structure-based conversion of the coenzyme requirement of a short-chain dehydrogenase/reductase involved in bacterial alginate metabolism

Ryuichi Takase[†], Bunzo Mikami[‡], Shigeyuki Kawai[†], Kousaku Murata[†,§], and Wataru Hashimoto[†,*]

[†]From the Laboratory of Basic and Applied Molecular Biotechnology, Division of Food Science and Biotechnology, Graduate School of Agriculture, Kyoto University, Uji, Kyoto 611-0011, Japan
[‡]From the Laboratory of Applied Structural Biology, Division of Applied Life Sciences, Graduate School of Agriculture, Kyoto University, Uji, Kyoto 611-0011, Japan
[§]Present address: Faculty of Science and Engineering, Setsunan University, Neyagawa, Osaka 572-8508, Japan

Running title: *Structural determinants for coenzyme requirement*

[*]To whom correspondence should be addressed: Wataru Hashimoto
Address: Laboratory of Basic and Applied Molecular Biotechnology, Division of Food Science and Biotechnology, Graduate School of Agriculture, Kyoto University, Uji, Kyoto 611-0011, Japan,
Tel: +81-774-38-3756; Fax number: +81-774-38-3767; E-mail: whasimot@kais.kyoto-u.ac.jp

Keywords: Alginate; Bacterial metabolism; Coenzyme requirement; Enzyme mechanisms; Kinetics; Short-chain dehydrogenase/reductase; Site-directed mutagenesis; X-ray crystallography

Background: NADPH-dependent α-keto acid reductase, belonging to the short-chain dehydrogenase/reductase family, is involved in bacterial alginate metabolism.
Results: A novel NADH-dependent α-keto acid reductase was identified and its tertiary structure was determined by X-ray crystallography.
Conclusion: Two short and long loops are structural determinants for coenzyme specificity.
Significance: A method for structure-based conversion of a coenzyme requirement was established.

ABSTRACT

The alginate-assimilating bacterium, *Sphingomonas* sp. strain A1, degrades the polysaccharide to monosaccharides through four alginate lyases reactions. The resultant monosaccharide, which is nonenzymatically converted to 4-deoxy-L-*erythro*-5-hexoseulose uronate (DEH), is further metabolized to 2-keto-3-deoxy-D-gluconate by NADPH-dependent reductase A1-R in the short-chain dehydrogenase/reductase (SDR) family. A1-R-deficient cells produced another DEH reductase, designated A1-R′, with a preference for NADH. Here we show the identification of a novel NADH-dependent DEH reductase A1-R′ in strain A1, structure determination of A1-R′ by X-ray crystallography, and structure-based conversion of a coenzyme requirement in SDR enzymes, A1-R and A1-R′. A1-R′ was purified from strain A1 cells and enzymatically characterized. Except for coenzyme requirement, there was no significant difference in enzyme characteristics between A1-R and A1-R′. Crystal structures of A1-R′ and A1-R′/NAD^+ complex were determined at 1.8 and 2.7 Å resolutions, respectively. Because of a 64% sequence identity, overall structures of A1-R′ and A1-R were similar, although a difference in the coenzyme-binding site (particularly nucleoside ribose 2′ region) was observed. Distinct from A1-R, A1-R′ included a negatively charged, shallower binding site. These differences were caused by amino acid residues on the two loops around the site. The A1-R′ mutant with the two A1-R-typed loops maintained potent enzyme activity with specificity for NADPH rather than NADH, demonstrating that the two loops determine the coenzyme requirement and loop exchange is a promising method for conversion of coenzyme requirement in the SDR family.

Coenzymes NADH and NADPH are electron mediators and involved in oxidation/reduction enzymatic reactions, though their physiological roles are different in biological reactions (1). NADH, mainly used in catabolism, accepts electrons from nutrients and plays important roles in the production of bioenergy in the form of ATP. On the other hand, NADPH is involved in assimilation or antioxidation by its reducing power. In general, an oxidation/reduction-catalytic enzyme shows specificity for either coenzyme based on their biological roles.

Recently, biofuel production from unused and/or excess biomass has been an area of interest (2). To achieve bioproduction, metabolic pathways are modified through introduction and/or disruption of certain genes. This biotechnology, called synthetic biology, is now being developed in academia and industry (3). However, oxidation/reduction reactions are strictly regulated in innate organisms, with coenzyme balance properly maintained. In the case of microbial production of useful substances, intracellular oxidation/reduction imbalance of coenzymes occurs because of the artificial improvement and/or addition of metabolic reactions. The imbalance often causes low-yield production. Two attempts have been conducted to solve this problem. One is to regenerate each coenzyme by coupling reactions using dehydrogenases of formate or glucose (4), and the other is to convert the coenzyme requirement of metabolic enzymes such as xylose reductase (5). The latter method is suitable for continuous production because addition of substrates such as formate/glucose and introduction of coenzyme-regenerating enzymes are unnecessary.

A lot of studies have been carried out to convert the coenzyme requirement. However, in many cases, resulting mutants show low enzyme activity compared with the wild-type (WT) enzyme (6-27). There are some successful cases (28-36), although general methods for conversion of the coenzyme requirement are being sought.

Alginate is a heteropolysaccharide consisting of two uronates β-D-mannuronate and α-L-guluronate (37). The polysaccharide is abundant as a major component of the cell wall

matrix in marine algae, such as brown seaweeds. Currently, effective utilization of marine biomass alginate is desirable because brown seaweeds are readily cultivated and cause no serious competing interests for food-stuffs (38). The gram-negative bacterium, *Sphingomonas* sp. strain A1, directly uptakes alginate into the cytoplasm through a superchannel consisting of a cell-surface pit and ATP-binding cassette transporter (39,40). Alginate is degraded to monosaccharides by the action of cytoplasmic endotype alginate lyases A1-I, -II and -III, and exotype lyase A1-IV (41,42). All of the resultant monosaccharides are nonenzymatically converted to 4-deoxy-L-*erythro*-5-hexoseulose uronate (DEH). DEH is reduced to 2-keto-3-deoxy-D-gluconate (KDG) by NADPH-dependent reductase, A1-R (ID: SPH3227), and KDG is catabolized to glyceraldehyde 3-phosphate and pyruvate through subsequent reactions by KDG kinase and aldolase, respectively (Fig. 1A) (43).

Cells of recombinant strain A1, which harbor genes coding for ethanol fermentation, produce bioethanol from alginate (44). Ethanologenic bacteria or yeast that have been modified by the addition of multiple genes involved in alginate import and assimilation have been reported to convert sugars from brown macroalgae to bioethanol (45,46). To optimize the alginate metabolism for biofuel production, an NADH-dependent DEH reductase is also valuable and two desirable enzymes have been found in *Vibrio* species (45,46). However, the characteristics of these enzymes remain to be clarified.

A1-R belongs to the short-chain dehydrogenase/reductase (SDR) family. SDR family enzymes use NADPH or NADH as a cofactor to metabolize sugars, fatty acids, and steroids (47). From bacteria to humans, a large number of organisms produce SDR family enzymes. More than 120,000 enzymes in the SDR family are registered in UniProtKB (http://www.uniprot.org/help/uniprotkb), although crystal structures thus far analyzed are mutually similar (48). Structural determinants for the coenzyme requirement in DEH reductases are valuable to establish a basic biotechnology regarding molecular conversion of coenzyme specificity in SDR family enzymes. Increasingly larger amounts of structural data regarding enzymes and proteins are being deposited in the Protein Data Bank (PDB), in proportion to the progress in the field of structural biology. Structure-based biotechnology is expected to become an important part of post-structural biology. For example, the structure-based conversions of polysaccharide-degrading enzymes from the exo to the endo mode of action have been achieved (49,50).

This study deals with molecular identification of a novel NADH-dependent DEH reductase (A1-R′) as a member of the SDR family, structure determination of A1-R′ and its complex with NAD^+, and the structure-based conversion of its coenzyme requirement.

EXPERIMENTAL PROCEDURES

Materials– Sodium alginate (viscosity of 1% (w/v) solution; 1000 cps) and hydroxylapatite were purchased from Nacalai Tesque. TOYOPEARL DEAE-650M and TOYOPEARL Butyl-650M were from Tosoh. HiLoad 26/10 Q Sepharose HP, HiLoad 16/60 Superdex 75 pg, HiLoad 16/60 Superdex 200 pg, and MonoQ HR 5/5 were from GE Healthcare. Restriction endonucleases and PCR-related enzymes were from Toyobo. Amicon Ultra-4 centrifugal filters were from Millipore. Bio-Gel P-2 was from Bio-Rad Laboratories. Other analytical grade chemicals were obtained from commercial sources.

Microorganisms and Culture Conditions– Strain A1 cells were routinely cultured at 30°C in minimal medium containing 0.5% (w/v) sodium alginate, 0.1% (w/v) $(NH_4)_2SO_4$, 0.1% (w/v) KH_2PO_4, 0.1% (w/v) Na_2HPO_4, 0.01% (w/v) yeast extract, and 0.01% (w/v) $MgSO_4 \cdot 7H_2O$. As a host for plasmid amplification, *Escherichia coli* strain DH5α (Toyobo) was routinely cultured aerobically at 37°C in LB medium [1% (w/v) tryptone, 0.5% (w/v) yeast extract, and 1% (w/v) NaCl] (pH 7.2) containing appropriate antibiotics.

Enzyme and Protein Assays– The DEH-reducing activity was assayed at 30°C in a standard reaction mixture (0.5 mL) consisting of 4 mM DEH, 0.2 mM coenzyme (NADH or NADPH), 50 mM potassium phosphate buffer (KPB) (pH 7.0), and appropriate amount of enzyme.

The activity was measured by continuously monitoring the decrease of absorbance at 340 nm, which corresponds to the oxidation of NADH or NADPH. One unit (U) of enzymatic activity was defined as the amount of enzyme required to oxidize 1 μmol of coenzyme per min at 30°C. The protein content was

determined according to the Bradford procedure (51), with bovine serum albumin as the standard. The kinetic parameters (k_{cat} and K_m) for coenzyme or DEH were determined with data from enzyme assays conducted with various concentrations of coenzyme or DEH using the Michaelis–Menten equation with the *kaleidaGraph* program (Synergy Software).

Construction of A1-R-deficient Strain A1– The strain A1 mutant with a deficiency in A1-R was generated through homologous recombination. Several plasmids were constructed to modify the strain A1 genome (Fig. 2). To amplify A1-R gene with upstream and downstream 500 bp regions, PCR was performed using A1-R±500 primers. Each primer used in this study is listed in Table 1. A reaction mixture (50 μL) contains 1 U of KOD-FX (Toyobo), 50 ng of strain A1 genomic DNA, 15 pmol each of primers, 20 nmol of dNTPs, and KOD-FX buffer (Toyobo). The PCR conditions were as follows: 94°C for 2 min, and then 20 cycles at 98°C for 10 s, 66°C for 30 s, and 68°C for 2 min. The resultant DNA fragments were ligated with *Hin*cII-digested pUC119 (Takara Bio). The resultant plasmid was designed as pUC119/A1-R±500. To mutate Gly-38 to Asp in pUC119/A1-R±500, A1-R_G38D primers were used and the resultant plasmid was designated pUC119/A1-R±500(G38D). Inverse PCR was performed with A1-R_XhoI primers to insert an *Xho*I recognition site after the stop codon of the A1-R gene. The resultant plasmid after phosphorylation and self-ligation was designated as pUC119/A1-R±500(G38D)_XhoI. The tetracycline resistance gene cassette from pACYC184 (NIPPON GENE) was inserted into the *Xho*I site of pUC119/A1-R±500(G38D)_XhoI and the resultant plasmid was designated pUC119/A1-R±500(G38D)_Tet. The plasmid was digested with *Pvu*II and *Eco*RI, and the resultant fragment, including the A1-R gene, was inserted into *Pvu*II and *Eco*RI-digested pKTY320 (52). The resulting plasmid was designated pKTY320/A1-R±500(G38D)_Tet. DH5α cells transformed with pKTY320/A1-R±500(G38D)_Tet were used as a donor. *E. coli* strain HB101 cells transformed with pRK2013 were used as a helper. To obtain an A1-R-deficient strain A1 mutant, triparental mating (53) was performed using three types of strain A1, donor, and helper. Strain A1 cells were cultured in 0.5% (w/v) alginate minimal medium. Donor cells were cultured in LB medium containing 100 μg mL^{-1} sodium ampicillin and 20 μg mL^{-1} tetracycline hydrochloride. Helper cells were cultured in LB medium containing 20 μg mL^{-1} kanamycin sulfate. Each of the bacterial cells was cultured to an exponential growth phase until turbidity at 600 nm reached 0.5–1.0. When turbidity was 1.0, the cell concentration in the culture was regarded as 1.0×10^9 cells mL^{-1}. Bacterial cells were collected and concentrations adjusted to 2×10^8 strain A1 cells, 1×10^8 donor cells, and 0.4×10^8 helper cells. All cells were collected at 25°C by centrifugation at 2,500 ×*g* for 5 min and washed with 500 μL of 10 mM $MgCl_2$. After centrifugation, bacterial cells were resuspended in 50 μL of 10 mM $MgCl_2$ and spotted onto a 0.2-μm pore size membrane filter placed on a 0.5% (w/v) alginate medium plate containing 0.5% (w/v) yeast extract. After incubating overnight at 30°C, bacterial cells on the filter were resuspended in 70 μL of 10 mM $MgCl_2$. The cell suspension was spread on a 0.5% (w/v) alginate minimal medium plate containing 20 μg mL^{-1} tetracycline hydrochloride. After incubation at 30°C for 4 days, single colonies were subjected to streak culture on a fresh alginate minimal medium plate containing tetracycline hydrochloride. As a result, ampicillin-sensitive and tetracycline-resistant cells were obtained. The nucleotide sequence of mutated and inserted regions in the strain A1 mutant genome was confirmed by dideoxy chain termination (54) using an automated DNA sequencer (Model 3730xl; Applied Biosystems). In the strain A1 mutant genome, the A1-R gene was substituted for the A1-R_G38D gene together with a tetracycline resistance gene.

Purification of Novel DEH Reductase from Strain A1– A novel DEH reductase A1-R′ was purified from strain A1 cells as follows. Unless otherwise specified, all procedures were performed at 4°C. Strain A1 cells were aerobically cultured in 6 L of 0.5% (w/v) alginate minimal medium (1.5 L per flask) at 30°C for 48 h, collected by centrifugation at 6,000 ×*g* for 5 min, and resuspended in 40 mL of 20 mM Tris-HCl (pH 7.5). Cells were ultrasonically disrupted (Insonator Model 201M; Kubota) at 9 kHz for 20 min, and the clear solution obtained after centrifugation at 20,000 ×*g* for 20 min was dialyzed against 1.5 L of 20 mM Tris-HCl (pH 7.5) twice and used as the cell extract. The cell extract was applied to a TOYOPEARL DEAE-650M column (6 ×

10 cm) previously equilibrated with 20 mM Tris-HCl (pH 7.5). After washing with 20 mM Tris-HCl (pH 7.5), the absorbed proteins were eluted with a linear gradient of NaCl (0–500 mM) in 20 mM Tris-HCl (pH 7.5, 600 mL), with a 10–mL fraction collected every 10 min. DEH-reducing activity was assayed in the presence of NADH or NADPH for all fractions. Fractions including DEH-reducing activities in the presence of NADH are called active fractions hereafter. The active fractions, eluted with 200–300 mM NaCl, were dialyzed against 1.5 L of 20 mM Tris-HCl (pH 7.5) twice. The resultant dialysate was saturated with 30% $(NH_4)_2SO_4$ and applied to a TOYOPEARL Butyl-650M column (3 × 20 cm) previously equilibrated with 20 mM Tris-HCl (pH 7.5) containing 30% saturated $(NH_4)_2SO_4$. After washing with 20 mM Tris-HCl (pH 7.5) containing 30% saturated $(NH_4)_2SO_4$, the absorbed proteins were eluted with a linear gradient of saturated $(NH_4)_2SO_4$ (30%–0%, 200 mL), with a 6 mL fraction collected every 6 min. The active fractions, eluted with 10%–0% saturated $(NH_4)_2SO_4$, were combined and dialyzed against 1.5 L of 20 mM Tris-HCl (pH 7.5) twice. The dialysate was concentrated to 0.63 mL at a concentration of 20-mg protein mL^{-1} and applied to a HiLoad 16/60 Superdex 200 pg column (1.6 × 60 cm) previously equilibrated with 20 mM Tris-HCl (pH 7.5) containing 0.15 M NaCl. Proteins were eluted with the same buffer (120 mL) with a 2 mL fraction collected every 2 min. The active fractions were combined and dialyzed against 1.5 L of 20 mM KPB (pH 7.0) twice. The dialysate was applied to a Hydroxylapatite column (1 × 3 cm) previously equilibrated with 20 mM KPB (pH 7.0). After washing with 20 mM KPB (pH 7.0), the absorbed proteins were eluted with a linear gradient of KPB (20–200 mM, 10 mL), with a 0.5 mL fraction collected every minute. The active fractions obtained on elution with 50–100 mM KPB were dialyzed against 1.5 L of 20 mM Tris-HCl (pH 7.5) twice. The dialysate was applied to a Mono Q HR 5/5 column (0.5 × 5 cm) previously equilibrated with 20 mM Tris-HCl (pH 7.5). After washing with 20 mM Tris-HCl (pH 7.5), the absorbed proteins were eluted with a linear gradient of NaCl (0–500 mM, 5 mL) in 20 mM Tris-HCl (pH 7.5), with a 0.5 mL fraction collected every minute. The active fractions, obtained on elution with 10–100 mM NaCl, were combined and applied to a HiLoad 16/60 Superdex 75 pg column (1.6 × 60 cm) previously equilibrated with 20 mM Tris-HCl (pH 7.5) containing 0.15 M NaCl. Proteins were eluted with the same buffer (120 mL), with a 2 mL fraction collected every 2 min, and the active fractions were combined and dialyzed against 1.5 L of 20 mM Tris-HCl (pH 7.5) twice. The dialysate was applied to a HiLoad 26/10 Q Sepharose HP column (2.6 × 10 cm) previously equilibrated with 20 mM Tris-HCl (pH 7.5). After washing with 20 mM Tris-HCl (pH 7.5), the absorbed proteins were eluted with a linear gradient of NaCl (0–500 mM, 200 mL) in 20 mM Tris-HCl (pH 7.5), with a 3 mL fraction collected every minute. The active fractions, eluted with 200–250 mM NaCl, were combined and confirmed as homogeneous by SDS-PAGE. The purified proteins were dialyzed against 1.5 L of 20 mM Tris-HCl (pH 7.5) twice and used as the native A1-R′ (nA1-R′).

Overexpression of A1-R′– The overexpression system for A1-R′ was constructed in *E. coli* cells as follows. To clone the A1-R′ gene, PCR was performed in a reaction mixture (50 μL) containing 1 U of KOD-Plus-Neo (Toyobo), 50 ng of strain A1 genomic DNA, 15 pmol each of forward and reverse primers, 10 nmol of dNTPs, 75 nmol of $MgCl_2$, and KOD-Plus-Neo buffer (Toyobo). The 5′ end of the forward primer (A1-R′_NdeI) contains 15 bases homologous to 15 bases of pET21b (Novagen) from the *Nde*I site toward opposite direction to the *Bam*HI site. In addition, the reverse primer (A1-R′_BamHI) possesses the same 15 bases of pET21b from the *Bam*HI site toward opposite direction to the *Nde*I site. PCR conditions were as follows: 94°C for 2 min, followed by 30 cycles at 98°C for 10 s, 63°C for 30 s and 68°C for 1 min. The resultant fragment was ligated with *Nde*I and *Bam*HI-digested pET21b using the In-Fusion HD Cloning Kit (Clontech). The resulting plasmid, designated as pET21b/A1-R′, includes the complete sequence of the A1-R′ gene with the original start and stop codons. *E. coli* strain BL21(DE3) (Novagen) was transformed with pET21b/A1-R′ and used for overexpression of A1-R′.

Purification of Recombinant A1-R′ from E. coli Cells– Unless otherwise specified, all procedures were performed at 4°C. For expression, *E. coli* strain BL21(DE3) cells harboring pET21b/A1-R′ were aerobically cultured at 30°C in 3 L of LB medium (1.5 L per flask), containing 100 μg mL^{-1} sodium ampicillin. When the turbidity at 600 nm

reached 0.6, isopropyl-β-D-thiogalactopyranoside was added to the culture at a final concentration of 0.4 mM, and the cells were further cultured at 16°C for 42 h. Cells were collected by centrifugation at 6,000 ×*g* for 5 min and resuspended in 30 mL of 20 mM Tris-HCl (pH 7.5). The cells were ultrasonically disrupted at 9 kHz for 20 min and the clear solution obtained on centrifugation at 20,000 ×*g* for 20 min was dialyzed against 1.5 L of 20 mM Tris-HCl (pH 7.5) twice. The dialysate was used as the cell extract. The recombinant A1-R′ (rA1-R′) was purified from the cell extract using four columns: TOYOPEARL DEAE-650M, TOYOPEARL Butyl-650M, HiLoad 26/10 Q Sepharose HP, and HiLoad 16/60 Superdex 200 pg. Each column was operated in the same way as described above.

Site-directed Mutagenesis– To construct multiple amino-acid substituted mutants or to insert the *Xho*I site, the KOD-Plus-Mutagenesis Kit (Toyobo) was used. Single amino-acid substituted mutants were constructed using a QuikChange Site-Directed Mutagenesis Kit (Stratagene). The plasmid pET21b/A1-R′ was used as a template for A1-R′ mutants. The plasmid pET21b/A1-R (43) was used for A1-R mutants. Mutations were confirmed by DNA sequencing as described above. Expression and purification of the mutants were performed in the same way as rA1-R′ from *E. coli*.

Crystallization and Structure Determination– The rA1-R′ solution was concentrated to 4.0 mL at a concentration of 31.1-mg protein mL^{-1} and crystallized by sitting-drop vapor diffusion on a 96-well Intelli-plate (Varitas). Commercial screening kits (Hampton Research, Emerald BioSystems, and Jena Bioscience) were used to search for the crystallization conditions of rA1-R′. The reservoir solution volume was 70 μL in each well, and the droplet was prepared by mixing 1 μL of the protein solution with 1 μL of the reservoir solution. Crystals of rA1-R′ in complex with NAD^+ (A1-R′/NAD^+) were prepared in the solution containing NAD^+ (Oriental Yeast). Each crystal of A1-R′ and A1-R′/NAD^+ picked off the nylon loop was directly placed in a cold nitrogen gas stream at −173°C. X-ray diffraction images of the crystals were collected at −173°C under the nitrogen gas stream and synchrotron radiation of wavelength 1.0000 Å at the BL-38B1 station of SPring-8 (Hyogo, Japan). Diffraction data were processed, merged, and scaled using the *HKL2000* program package (DENZO and SCALEPACK) (55). The structure of A1-R′ was determined by molecular replacement using coordinates of A1-R (PDB-ID, 3AFM) as an initial model using the *MOLREP* program (56), in the *CCP4* program package (57). Structure refinement was conducted using the *Refmac5* program (58). Randomly selected 5% reflections were excluded from refinement and used to calculate R_{free}. After each refinement cycle, the model was manually adjusted using the *Coot* program (59). Water molecules were incorporated where the difference in density exceeded 3.0σ in F_o–F_c map. Final model quality was checked using the *PROCHECK* program (60). Protein models were superimposed and their root-mean-square deviation (r.m.s.d.) was determined using the *LSQKAB* program (61), which is a part of *CCP4*. Coordinates used in this work were obtained from the Research Collaboratory for Structural Bioinformatics PDB. Figures of protein structures were prepared using the *PyMOL* program (62).

Analytical Methods– Polyacrylamide gel (12.5%) was used for SDS-PAGE. Proteins on the gel were stained with Coomassie Brilliant Blue R-250. DEH was prepared from sodium alginate by using exotype alginate lyase, Atu3025 (63), and purified using Centriprep centrifugal filter and Bio-Gel P-2 size-exclusion column as previously described (43). Thiobarbituric acid method (64) was used for determination of DEH concentration. N-terminal amino acid sequence of the enzyme was determined by an Edman degradation method (65). To evaluate structural folding of the enzymes in 50 mM KPB (pH 7.0), circular dichroism (CD) spectra were measured in the far ultraviolet region (260–190 nm) using a JASCO J-720C spectropolarimeter (JASCO) at 25°C. Samples were analyzed in a quartz cell with a path length of 0.1 mm. The content of helix and strand in the enzymes was estimated using the program *CDPro* (http://lamar.colostate.edu/~sreeram/CDPro/main.html). Structural folding in the enzymes was also investigated by measuring their thermal stabilities using differential scanning fluorimetry (DSF) as previously described (66).

RESULTS

DEH-reducing Activity in A1-R-deficient Strain A1– To investigate the physiological

significance of A1-R in strain A1, the strain A1 mutant (MT) with a deficiency in A1-R was constructed and characterized. The MT cells seem to produce A1-R_G38D instead of native A1-R. In A1-R_G38D, Gly-38 was replaced with Asp. In our previous paper (43), residue Gly-38 was found to be important for accommodating the phosphate group of NADPH due to its lack of side chain. In fact, the mutant (A1-R_G38D) with Gly-38 substituted with Asp exhibited a significantly reduced enzyme activity toward NADH (k_{cat}, 8.29 s^{-1}; K_m, 181 μM) as well as NADPH (k_{cat}, 5.16 s^{-1}; K_m, 178 μM). The specific activity of purified A1-R_G38D with 0.2 mM NADPH was drastically decreased to 1/24 (17.2 U mg^{-1}) that of the native A1-R (406 U mg^{-1}). This means that the strain A1 MT, which produces the A1-R_G38D mutant, shows negligible DEH reductase activity even in the presence of NADPH and NADH. MT cells showed little growth in 0.5% (w/v) alginate minimal medium containing 20 μg mL^{-1} tetracycline hydrochloride, although cell growth was observed after several acclimatizations. Specific DEH-reducing activities in strain A1 wild-type and MT cell extracts were measured with 0.2 mM NADPH. The activity in the cell extract of MT corresponded to half as much as that of WT. The MT cell extract showed higher activity with 0.2 mM NADH than with NADPH. These results suggest the existence of another DEH reductase with a preference for NADH.

Identification of Another Novel DEH Reductase– A novel DEH reductase, termed A1-R′, with a preference for NADH was purified 234-fold from strain A1 cells through seven steps of column chromatography with recovery of 1.35% (Table 2). The purified native A1-R′ (nA1-R′) was homogeneous by SDS-PAGE (Fig. 3A, left). The N-terminal amino acid sequence of the purified enzyme was determined to be "NH_2-Met-Phe-Ser-Asp-Leu." In a genome database search of strain A1 (67), this protein was assigned to ID: SPH1210.

Based on the primary structure, the molecular weight of A1-R′ was calculated to be 27,337, with 258 amino acid residues. The sequence similarity between A1-R′ and A1-R was compared using CLUSTALW (http://clustalw.ddbj.nig.ac.jp/) and the resultant score was high, with 64% identity (Fig. 4A). BLAST search (http://blast.ncbi.nlm.nih.gov/Blast.cgi) indicates that A1-R′ shows a high sequence identity (40%–71%) with an SDR family enzyme, 3-ketoacyl-CoA reductase. A1-R′ includes a glycine-rich motif of the cofactor-binding Rossmann fold region (13-TGXXXGXG-20) and catalytic triad residues (Ser-150, Tyr-164, and Lys-168) conserved in the SDR family (Fig. 4B). These results demonstrate that A1-R′ belongs to the SDR family.

Enzymatic Properties of A1-R′– Properties of nA1-R′ are as follows:

(i) Molecular mass. The molecular mass of nA1-R′ was estimated to be 25 kDa via SDS-PAGE (Fig. 3A, left). Elution volume of nA1-R′ after HiLoad 16/60 Superdex 200 pg size exclusion chromatography showed that the molecular mass of nA1-R′ is approximately 110 kDa (data not shown). These results indicated that nA1-R′ exists as a homotetramer.

(ii) Optimal pH, optimal temperature, and thermal stability. nA1-R′ was the most active at pH 6.5 (KPB) and 51°C. The activity decreased by half after preincubation at 42°C for 5 min (Fig. 3B).

(iii) Chemicals. The DEH-reduction reaction was conducted at 30°C in the presence or absence of different compounds, such as thiol reagents, the chelator EDTA, sugars, and metals. Almost all the chemicals tested had no significant effect (76%–121%) on the reaction of nA1-R′ (Table 3).

(iv) Kinetic parameters. Kinetic parameters of nA1-R′ were determined based on the saturation curve of enzyme activities at various concentrations of substrates (Table 4). k_{cat} and K_m values were 227 s^{-1} and 4790 μM toward DEH; 280 s^{-1} and 15.5 μM toward NADH; and 233 s^{-1} and 224 μM toward NADPH. k_{cat} scores toward NADH and NADPH were similar, although the affinity for NADH was 14.5-fold higher compared with that for NADPH. This indicates that A1-R′ shows a preference for NADH.

rA1-R′ from E. coli– rA1-R′ was purified to 1.62-fold from recombinant *E. coli* cells through four steps of column chromatography (Table 2). rA1-R′ was homogeneous via SDS-PAGE (Fig. 3A, right). Kinetic parameters of rA1-R′ were comparable with those of nA1-R′.

Crystal Structure of A1-R′– A1-R′ and A1-R were very similar except for their coenzyme requirements, suggesting that local structural differences cause these variations. X-ray crystallography of A1-R′ was conducted

to clarify structural determinants for the coenzyme requirement. An A1-R′ crystal was obtained in a droplet consisting of 20% (v/v) polyethylene glycol 400, 0.05 M Na/K phosphate (pH 6.2), 0.1 M NaCl, and 15.6 mg mL^{-1} rA1-R′. The crystal structure of A1-R′ was determined at a resolution of 1.80 Å by the molecular replacement method. After refinement, R- and R_{free}-factors were 18.2% and 20.2%, respectively. Data collection and refinement statistics are summarized in Table 5. The refined model had two identical monomers in an asymmetric unit, termed molecules A and B. One phosphate molecule was bound to molecule A, and two phosphate molecules were bound to molecule B. Residues 1 and 199–212 of molecule A, and residues 1 and 197–213 of molecule B were unable to be assigned because the residues in this region of the electron density map are disordered. These residues are considered to form a long flexible loop. Structures of molecules A and B are basically identical because the r.m.s.d. between both was calculated as 0.232 Å. A1-R′ has 10 α-helices and seven β-strands, and consists of a three-layered structure, α/β/α, with a coenzyme-binding site, called Rossmann fold (68) (Figs. 4B, 5A, B). The overall structure of A1-R′ mimics that of A1-R (Fig. 5A, B). The torsion angle of Thr-141 peptide bond was the outlier in the Ramachandran plot analysis. Thr-141 is on the loop consisting of only three residues between parallel α-helix H5 and β-strand S5. As a result, Thr-141 forms a hydrogen bond with Ser-139, and the loop is drastically bent.

Catalytic Triad in A1-R′– Based on the sequence alignment (Fig. 4B), Ser-150, Tyr-164, and Lys-168 of A1-R′ are suggested to function as a catalytic triad. To confirm their roles as catalytic residues, three A1-R′ mutants (S150A, Y164F, and K168A, in which Ser-150, Tyr-164, and Lys-168 were replaced with Ala, Phe, and Ala, respectively) were constructed by site-directed mutagenesis. The mutants were purified in the same way as WT rA1-R′ and their kinetic parameters (k_{cat} and K_m) for DEH were determined as follows: WT, 201 s^{-1} and 5.68 mM; S150A, 0.00257 s^{-1} and 13.3 mM; Y164F, 0.000307 s^{-1} and 21.2 mM; and K168A, 0.373 s^{-1} and 5.07 mM. Compared with WT rA1-R′, all the mutants significantly decreased the enzymatic activity (k_{cat} K_m^{-1}) (S150A, 0.00054%; Y164F, 0.000040%; K168A, 0.21%). In particular, Y164F decreased the k_{cat} value drastically to 0.000000015%.

The arrangement of each residue of the catalytic triad (Ser-150, Tyr-164, and Lys-168) in the crystal structure of A1-R′ was identical to that of many SDR family enzymes, e.g., 3α,20β-hydroxysteroid dehydrogenase (PDB-ID, 2HSD). Because the involvement of the catalytic triad in the reactions catalyzed by SDR family enzymes has been well documented (47,48,69), the roles of Ser-150, Tyr-164, and Lys-168 in the A1-R′ reaction were postulated based on structural comparison with enzymes of the well-characterized SDR family as follows: Ser-150 stabilizes the reaction intermediates, Tyr-164 acts as a catalytic base in the reduction reaction, and Lys-168 is crucial for the proper orientation of the coenzyme and lowering the pK_a of Tyr-164.

Binding Mode to Coenzyme– To clarify the structural difference of the coenzyme-binding mode between A1-R′ and A1-R, the A1-R′/NAD^+ complex crystal was obtained in the solution containing 0.85% (v/v) polyethylene glycol 400, 0.85 M $(NH_4)_2SO_4$, 43 mM sodium 4-(2-hydroxyethyl)-1-piperazineethanesulfonic acid (pH 7.5), 15.6 mg mL^{-1} rA1-R′, and 0.5 mM NAD^+. The initial phase was determined by molecular replacement using coordinates of the ligand-free A1-R′ as a search model. After refinement, final structure was determined at 2.67 Å. Two monomers, termed molecules A and B, were present in an asymmetric unit. In molecule B, NAD^+ bound to Rossmann fold (Fig. 5C, D). In addition, four sulfate molecules were bound to molecule A, and one sulfate molecule was bound to molecule B. Residues 198–213 of molecule A and residues 197–213 of molecule B were unable to be assigned because the residues in this region of the electron density map are disordered. The r.m.s.d. value between molecules A and B of A1-R′/NAD^+ was calculated as 0.314 Å, demonstrating that there is no significant conformational change between NAD^+-free and -bound A1-R′s.

The coenzyme-binding site of A1-R′ was compared with that of A1-R (Fig. 6A, B). In particular, the residues around nucleoside ribose 2′ region of coenzyme bound were different between A1-R′ and A1-R, postulating that these are involved in coenzyme specificity. The electric charge of the molecular surface at pH 7.0 around the coenzyme-binding site of A1-R′ and A1-R is shown in Figure 6C, D. In A1-R′/NAD^+, the A1-R′ site bound to the nucleoside ribose 2′ region of the coenzyme is

negatively charged by the influence of Glu-17. On the other hand, the corresponding site in A1-R is positively charged by Arg-39 and Lys-40. Negative electric charge of Glu-17 may cause electrostatic repulsion to nucleoside ribose 2′ phosphate group of NADPH. On the other hand, the positive charge of Arg-39 and Lys-40 is considered to cause electrostatic attraction. The space in A1-R′ is shallower compared with that in A1-R. The difficulty in binding of NADPH to A1-R′ is partly because of this smaller space at the nucleoside ribose 2′-binding site.

Conversion of Coenzyme Requirement– The residues involved in electric charge and space formation at the binding site of the nucleoside ribose 2′ region of the coenzyme are on the two loops. In A1-R′, the short and long loops are composed of 5 residues (13-TGSTE-17) and 7 residues (37-NSHVDPA-43), respectively (Fig. 6E). It was suggested that these two loops determine the coenzyme requirement because both A1-R′ and A1-R were very similar except for this requirement. To assess this hypothesis, A1-R′ and A1-R mutants were constructed, in which the loops were mutually exchanged. The terms "ex_S," "ex_L," and "ex_W" mean the mutants in which short loop, long loop, and both loops were exchanged, respectively.

To validate the structural folding of the A1-R′ and A1-R mutants that have had their loop(s) exchanged, the purified mutants and the WT enzymes were subjected to CD spectroscopy (Fig. 7A, B). The CD spectrum of each mutant was comparable to that of the corresponding WT enzyme. Subsequently, the secondary structural elements were determined by analyzing the CD profiles using the program *CDPro*. No significant differences in secondary structure were observed between the WT and mutant enzymes. This CD analysis suggested that all the mutants were properly folded, in manners similar to those of their respective WT enzymes, and that the enzymatic activity of the mutants was influenced by mutation, not misfolding.

Kinetic parameters of the mutants for NADH, NADPH, and DEH were determined (Table 6) after purification in the same way as rA1-R′. There were no significant differences between the K_m values for DEH of the WT enzymes and those of the mutant enzymes as follows: WT A1-R′, 4.8 mM; A1-R′ mutants, 2.8–4.8 mM; WT A1-R, 1.9 mM; and A1-R mutants, 1.7–3.5 mM). These results suggest that the affinities of the mutants for the DEH substrate were comparable with those of their respective WT enzymes.

Both A1-R′_ex_S and A1-R′_ex_L increased affinity with NADPH. A1-R′_ex_W synergistically increased affinity with NADPH, although these three A1-R′ mutants displayed a decreased k_{cat} for NADPH compared with that for WT A1-R′. These results suggest that the two loops play a key role in affinity with NADPH. A1-R′_ex_W drastically increased the k_{cat} K_m^{-1} value for NADPH, while its k_{cat} K_m^{-1} value for NADH decreased, indicating that A1-R′_ex_W showed an 85-fold preference for NADPH, compared with NADH. Moreover, kinetic parameters of A1-R′_ex_W for NADPH were comparable with those of A1-R for NADPH. In contrast to conversion in dependence from NADH to NADPH, three A1-R mutants exhibited decreased activity for NADH compared with that for WT A1-R.

DISCUSSION

A novel NADH-dependent DEH reductase, A1-R′, was identified in strain A1. To date, two NADH-dependent DEH reductases from vibrios have been reported (45,46), although their enzyme properties and structures remain to be clarified. This is the first report on structure/function relationships of NADH-dependent DEH reductase and complete conversion of the coenzyme requirement in the enzyme.

Previously, Tomita *et al*. succeeded in converting the coenzyme requirement in the non SDR family enzyme, malate dehydrogenase (MDH), by multiple site-directed mutagenesis (30). Exchange of one of the MDH loops corresponding to the A1-R′ loops also contributes to conversion of coenzyme requirement, although the loop mutant exhibited a reduced enzyme activity (k_{cat} K_m^{-1}) compared with the WT enzyme. Recently, Brinkmann-Chen *et al*. established a method for conversion of the coenzyme requirement in the non SDR family enzymes, ketol-acid reductoisomerase family enzymes, through mutation of some residues in a loop and succeeding random mutations (36).

Conversion of the coenzyme requirement in A1-R′ was achieved by exchange of two loops close to the coenzyme-binding site. The A1-R′ mutant with A1-R-typed loops showed a high k_{cat} score and low K_m value for NADPH, corresponding to those of A1-R for NADPH. From these results, it was revealed that the

nature of the two loops determines the coenzyme requirement. Because SDR family enzymes commonly have the two loops in the Rossmann fold, the exchange of the two loops is expected to be a potential method to convert the coenzyme requirement of other SDR enzymes. The SDR family includes several metabolic enzymes, and thus the regulation of the coenzyme requirement will enable maintenance of the cellular oxidation/reduction balance. Well-balanced coenzyme concentration can lead to high-efficiency and continuous production of useful chemicals.

It is of interest that NADPH-dependent A1-R′_ex_W showed high activity, whereas NADH-dependent A1-R_ex_W showed low activity (Table 6). Therefore, the tertiary and quaternary structures of A1-R′_ex_W and A1-R_ex_W were determined by X-ray crystallography, even though no significant difference in secondary structure was observed between the WT enzymes and their respective mutants by CD spectroscopy. The overall structures of A1-R′_ex_W and A1-R_ex_W superimposed well on those of WT A1-R′ and A1-R, respectively (Fig. 7C, D), indicating that the structural folding of both mutants was identical to that of their respective WT enzymes. The significant decrease in enzymatic activity exhibited by A1-R_ex_W is probably due to the exchange of the two loops, not to misfolding. The A1-R′-type loop(s) were considered to be unsuitable for interaction with the basic scaffold of A1-R. In fact, the loop mutants A1-R_ex_W and A1-R_ex_L were found to be less thermally stable than WT A1-R through DSF analysis. The fluorescence of SYPRO Orange that bound to denatured proteins was measured during heat treatment (from 25°C to 95°C). The melting temperatures, T_m, of the WT and mutant enzymes were determined as the transition midpoint in the fluorescence profile. The fluorescence profiles of A1-R_ex_W (T_m, 49.2°C) and A1-R_ex_L (T_m, 47.8°C) were significantly shifted to a lower temperature, compared with that of WT A1-R (T_m, 55.6°C) (Fig. 7F), suggesting that WT A1-R was thermally more stable than the mutants. On the other hand, the T_m (42.7°C) of A1-R′_ex_W was slightly lower than that (T_m, 45.7°C) of WT A1-R′ (Fig. 7E).

The question as to why strain A1 has two different DEH reductases will be the focus of future studies. DEH is demonstrated to be toxic to bacterial cells (70), suggesting that strain A1 cells are obliged to reduce DEH immediately to detoxify and metabolize alginate, although the intracellular NAD^+/NADH ratio is influenced by the outer environment (i.e., oxygen concentration). To reduce DEH under any circumstance, strain A1 may have two types of reductases with different coenzyme requirements. In the case of a high level of NADH, strain A1 cells reduce DEH by A1-R′ and conserve NADPH for assimilation. As intracellular levels of NADH decrease, A1-R may reduce DEH using NADPH.

REFERENCES

1. Moat, A. G., and Foster, J. W. (1987) Biosynthesis and salvage pathways of pyridine nucleotide. *in* Pyridine Nucleotide Coenzymes Part A (D. D. O. Avramovic & R. Poulson eds.). *John Wiley & Sons, Inc., New York*, 1-24
2. Vertès, A. A., Qureshi, N., Blaschek, H. P., and Yukawa, H. (2010) Front Matter. *Strategies for Global Industries: Biomass to Biofuels*, 1-22
3. Colin, V. L., Rodriguez, A., and Cristobal, H. A. (2011) The role of synthetic biology in the design of microbial cell factories for biofuel production. *J. Biomed. Biotechnol.* **2011**, 601834
4. Kaup, B., Bringer-Meyer, S., and Sahm, H. (2004) Metabolic engineering of *Escherichia coli*: construction of an efficient biocatalyst for D-mannitol formation in a whole-cell biotransformation. *Appl. Microbiol. Biotechnol.* **64**, 333-339
5. Watanabe, S., Saleh, A. A., Pack, S. P., Annaluru, N., Kodaki, T., and Makino, K. (2007) Ethanol production from xylose by recombinant *Saccharomyces cerevisiae* expressing protein engineered $NADP^+$-dependent xylitol dehydrogenase. *J. Biotechnol.* **130,** 316-319
6. Galkin, A., Kulakova, L., Ohshima, T., Esaki, N., and Soda, K. (1997) Construction of a new leucine dehydrogenase with preferred specificity for $NADP^+$ by site-directed mutagenesis of the strictly NAD^+-specific enzyme. *Protein Eng.* **10**, 687-690
7. Petschacher, B., Leitgeb, S., Kavanagh, K. L., Wilson, D. K., and Nidetzky, B. (2005) The coenzyme specificity of *Candida tenuis* xylose reductase (AKR2B5) explored by site-directed mutagenesis and X-ray crystallography. *Biochem. J.* **385**, 75-83
8. Clermont, S., Corbier, C., Mely, Y., Gerard, D., Wonacott, A., and Branlant, G. (1993) Determinants of coenzyme specificity in glyceraldehyde-3-phosphate dehydrogenase: role of the acidic residue in the fingerprint region of the nucleotide binding fold. *Biochemistry* **32**, 10178-10184
9. Banta, S., Swanson, B. A., Wu, S., Jarnagin, A., and Anderson, S. (2002) Alteration of the specificity of the cofactor-binding pocket of *Corynebacterium* 2,5-diketo-D-gluconic acid reductase A. *Protein Eng.* **15**, 131-140
10. Holmberg, N., Ryde, U., and Bulow, L. (1999) Redesign of the coenzyme specificity in L-lactate dehydrogenase from *Bacillus stearothermophilus* using site-directed mutagenesis and media engineering. *Protein Eng.* **12**, 851-856
11. Yaoi, T., Miyazaki, K., Oshima, T., Komukai, Y., and Go, M. (1996) Conversion of the coenzyme specificity of isocitrate dehydrogenase by module replacement. *J. Biochem.* **119**, 1014-1018
12. Rane, M. J., and Calvo, K. C. (1997) Reversal of the nucleotide specificity of ketol acid reductoisomerase by site-directed mutagenesis identifies the NADPH binding site. *Arch. Biochem. Biophys.* **338**, 83-89
13. Shiraishi, N., Croy, C., Kaur, J., and Campbell, W. H. (1998) Engineering of pyridine nucleotide specificity of nitrate reductase: mutagenesis of recombinant cytochrome b reductase fragment of *Neurospora crassa* NADPH:Nitrate reductase. *Arch. Biochem. Biophys.* **358**, 104-115
14. Eppink, M. H., Overkamp, K. M., Schreuder, H. A., and Van Berkel, W. J. (1999) Switch of coenzyme specificity of *p*-hydroxybenzoate hydroxylase. *J. Mol. Biol.* **292**, 87-96
15. Elmore, C. L., and Porter, T. D. (2002) Modification of the nucleotide cofactor-binding site of cytochrome P-450 reductase to enhance turnover with NADH *in vivo*. *J. Biol. Chem.* **277**, 48960-48964
16. Kristan, K., Stojan, J., Adamski, J., and Lanisnik Rizner, T. (2007) Rational design of novel mutants of fungal 17 β-hydroxysteroid dehydrogenase. *J. Biotechnol.* **129**, 123-130
17. Dambe, T. R., Kuhn, A. M., Brossette, T., Giffhorn, F., and Scheidig, A. J. (2006) Crystal structure of NADP(H)-dependent 1,5-anhydro-D-fructose reductase from *Sinorhizobium morelense* at 2.2 Å resolution: construction of a NADH-accepting mutant and its application in rare sugar synthesis. *Biochemistry* **45**, 10030-10042
18. Medina, M., Luquita, A., Tejero, J., Hermoso, J., Mayoral, T., Sanz-Aparicio, J., Grever, K., and Gomez-Moreno, C. (2001) Probing the determinants of coenzyme specificity in ferredoxin-$NADP^+$ reductase by site-directed mutagenesis. *J. Biol. Chem.* **276**,

11902-11912
19. Chen, R., Greer, A., and Dean, A. M. (1995) A highly active decarboxylating dehydrogenase with rationally inverted coenzyme specificity. *Proc. Natl. Acad. Sci. U.S.A.* **92**, 11666-11670
20. Hoelsch, K., Suhrer, I., Heusel, M., and Weuster-Botz, D. (2013) Engineering of formate dehydrogenase: synergistic effect of mutations affecting cofactor specificity and chemical stability. *Appl. Microbiol. Biotechnol.* **97**, 2473-2481
21. Bernard, N., Johnsen, K., Holbrook, J. J., and Delcour, J. (1995) D175 discriminates between NADH and NADPH in the coenzyme binding site of *Lactobacillus delbrueckii* subsp. *Bulgaricus* D-lactate dehydrogenase. *Biochem. Biophys. Res. Commun.* **208**, 895-900
22. Serov, A. E., Popova, A. S., Fedorchuk, V. V., and Tishkov, V. I. (2002) Engineering of coenzyme specificity of formate dehydrogenase from *Saccharomyces cerevisiae*. *Biochem. J.* **367**, 841-847
23. Capone, M., Scanlon, D., Griffin, J., and Engel, P. C. (2011) Re-engineering the discrimination between the oxidized coenzymes NAD^+ and $NADP^+$ in clostridial glutamate dehydrogenase and a thorough reappraisal of the coenzyme specificity of the wild-type enzyme. *FEBS J.* **278**, 2460-2468
24. Baroni, S., Pandini, V., Vanoni, M. A., and Aliverti, A. (2012) A single tyrosine hydroxyl group almost entirely controls the NADPH specificity of *Plasmodium falciparum* ferredoxin-$NADP^+$ reductase. *Biochemistry* **51**, 3819-3826
25. Lerchner, A., Jarasch, A., Meining, W., Schiefner, A., and Skerra, A. (2013) Crystallographic analysis and structure-guided engineering of NADPH-dependent *Ralstonia* sp. alcohol dehydrogenase toward NADH cosubstrate specificity. *Biotechnol. Bioeng.* **110**, 2803-2814
26. Scrutton, N. S., Berry, A., and Perham, R. N. (1990) Redesign of the coenzyme specificity of a dehydrogenase by protein engineering. *Nature* **343**, 38-43
27. Marohnic, C. C., Bewley, M. C., and Barber, M. J. (2003) Engineering and characterization of a NADPH-utilizing cytochrome b5 reductase. *Biochemistry* **42**, 11170-11182
28. Zhang, L., Ahvazi, B., Szittner, R., Vrielink, A., and Meighen, E. (1999) Change of nucleotide specificity and enhancement of catalytic efficiency in single point mutants of *Vibrio harveyi* aldehyde dehydrogenase. *Biochemistry* **38**, 11440-11447
29. Hsieh, J. Y., Liu, G. Y., Chang, G. G., and Hung, H. C. (2006) Determinants of the dual cofactor specificity and substrate cooperativity of the human mitochondrial $NAD(P)^+$-dependent malic enzyme: functional roles of glutamine 362. *J. Biol. Chem.* **281**, 23237-23245
30. Miller, S. P., Lunzer, M., and Dean, A. M. (2006) Direct demonstration of an adaptive constraint. *Science* **314**, 458-461
31. Tomita, T., Fushinobu, S., Kuzuyama, T., and Nishiyama, M. (2006) Structural basis for the alteration of coenzyme specificity in a malate dehydrogenase mutant. *Biochem. Biophys. Res. Commun.* **347**, 502-508
32. Watanabe, S., Kodaki, T., and Makino, K. (2005) Complete reversal of coenzyme specificity of xylitol dehydrogenase and increase of thermostability by the introduction of structural zinc. *J. Biol. Chem.* **280**, 10340-10349
33. Ehrensberger, A. H., Elling, R. A., and Wilson, D. K. (2006) Structure-guided engineering of xylitol dehydrogenase cosubstrate specificity. *Structure* **14**, 567-575
34. Chen, R., Greer, A., and Dean, A. M. (1996) Redesigning secondary structure to invert coenzyme specificity in isopropylmalate dehydrogenase. *Proc. Natl. Acad. Sci. U.S.A.* **93**, 12171-12176
35. Zheng, H., Bertwistle, D., Sanders, D. A., and Palmer, D. R. (2013) Converting NAD-specific inositol dehydrogenase to an efficient NADP-selective catalyst, with a surprising twist. *Biochemistry* **52**, 5876-5883
36. Brinkmann-Chen, S., Flock, T., Cahn, J. K., Snow, C. D., Brustad, E. M., McIntosh, J. A., Meinhold, P., Zhang, L., and Arnold, F. H. (2013) General approach to reversing ketol-acid reductoisomerase cofactor dependence from NADPH to NADH. *Proc. Natl. Acad. Sci. U.S.A.* **110**, 10946-10951

37. Gacesa, P. (1988) Alginates. *Carbohydr. polym.* **8**, 161-182
38. Stokstad, E. (2012) Biofuels. Engineered superbugs boost hopes of turning seaweed into fuel. *Science* **335**, 273
39. Hisano, T., Kimura, N., Hashimoto, W., and Murata, K. (1996) Pit structure on bacterial cell surface. *Biochem. Biophys. Res. Commun.* **220**, 979-982
40. Momma, K., Okamoto, M., Mishima, Y., Mori, S., Hashimoto, W., and Murata, K. (2000) A novel bacterial ATP-binding cassette transporter system that allows uptake of macromolecules. *J. Bacteriol.* **182**, 3998-4004
41. Yoon, H.-J., Hashimoto, W., Miyake, O., Okamoto, M., Mikami, B., and Murata, K. (2000) Overexpression in *Escherichia coli*, purification, and characterization of *Sphingomonas* sp. A1 alginate lyases. *Protein Expr. Purif.* **19**, 84-90
42. Hashimoto, W., Miyake, O., Momma, K., Kawai, S., and Murata, K. (2000) Molecular identification of oligoalginate lyase of *Sphingomonas* sp. strain A1 as one of the enzymes required for complete depolymerization of alginate. *J. Bacteriol.* **182**, 4572-4577
43. Takase, R., Ochiai, A., Mikami, B., Hashimoto, W., and Murata, K. (2010) Molecular identification of unsaturated uronate reductase prerequisite for alginate metabolism in *Sphingomonas* sp. A1. *Biochim. Biophys. Acta* **1804**, 1925-1936
44. Takeda, H., Yoneyama, F., Kawai, S., Hashimoto, W., and Murata, K. (2011) Bioethanol production from marine biomass alginate by metabolically engineered bacteria. *Energy Environ. Sci.* **4**, 2575–2581
45. Wargacki, A. J., Leonard, E., Win, M. N., Regitsky, D. D., Santos, C. N., Kim, P. B., Cooper, S. R., Raisner, R. M., Herman, A., Sivitz, A. B., Lakshmanaswamy, A., Kashiyama, Y., Baker, D., and Yoshikuni, Y. (2012) An engineered microbial platform for direct biofuel production from brown macroalgae. *Science* **335**, 308-313
46. Enquist-Newman, M., Faust, A. M. E., Bravo, D. D., Santos, C. N. S., Raisner, R. M., Hanel, A., Sarvabhowman, P., Le, C., Regitsky, D. D., Cooper, S. R., Peereboom, L., Clark, A., Martinez, Y., Goldsmith, J., Cho, M. Y., Donohoue, P. D., Luo, L., Lamberson, B., Tamrakar, P., Kim, E. J., Villari, J. L., Gill, A., Tripathi, S. A., Karamchedu, P., Paredes, C. J., Rajgarhia, V., Kotlar, H. K., Bailey, R. B., Miller, D. J., Ohler, N. L., Swimmer, C., and Yoshikuni, Y. (2013) Efficient ethanol production from brown macroalgae sugars by a synthetic yeast platform. *Nature* **505**, 239-243
47. Kavanagh, K. L., Jornvall, H., Persson, B., and Oppermann, U. (2008) Medium- and short-chain dehydrogenase/reductase gene and protein families: the SDR superfamily: functional and structural diversity within a family of metabolic and regulatory enzymes. *Cell. Mol. Life Sci.* **65**, 3895-3906
48. Persson, B., and Kallberg, Y. (2013) Classification and nomenclature of the superfamily of short-chain dehydrogenases/reductases (SDRs). *Chem. Biol. Interact.* **202**, 111-115
49. Proctor, M. R., Taylor, E. J., Nurizzo, D., Turkenburg, J. P., Lloyd, R. M., Vardakou, M., Davies, G. J., and Gilbert, H. J. (2005) Tailored catalysts for plant cell-wall degradation: redesigning the exo/endo preference of *Cellvibrio japonicus* arabinanase 43A. *Proc. Natl. Acad. Sci. U.S.A.* **102**, 2697-702
50. Ochiai, A., Itoh, T., Mikami, B., Hashimoto, W., and Murata, K. (2009) Structural determinants responsible for substrate recognition and mode of action in family 11 polysaccharide lyases. *J. Biol. Chem*., **284**, 10181-10189
51. Bradford, M. M. (1976) A rapid and sensitive method for the quantitation of microgram quantities of protein utilizing the principle of protein-dye binding. *Anal. Biochem.* **72**, 248-254
52. Kimbara, K., Hashimoto, T., Fukuda, M., Koana, T., Takagi, M., Oishi, M., and Yano, K. (1989) Cloning and sequencing of two tandem genes involved in degradation of 2,3-dihydroxybiphenyl to benzoic acid in the polychlorinated biphenyl-degrading soil bacterium *Pseudomonas* sp. strain KKS102. *J. Bacteriol.* **171**, 2740-2747
53. Ruvkun, G. B., and Ausubel, F. M. (1981) A general method for site-directed mutagenesis in prokaryotes. *Nature* **289**, 85-88
54. Sanger, F., Nicklen, S., and Coulson, A. R. (1977) DNA sequencing with chain-terminating inhibitors. *Proc. Natl. Acad. Sci. U.S.A.* **74**, 5463-5467
55. Otwinowski, Z., and Minor, W. (1997) Processing of X-ray diffraction data. *Methods*

Enzymol. **276**, 307-326
56. Vagin, A., and Teplyakov, A. (2010) Molecular replacement with MOLREP. *Acta Crystallogr. D Biol. Crystallogr.* **66**, 22-25
57. Collaborative Computational Project, N. (1994) The CCP4 suite: programs for protein crystallography. *Acta Crystallogr. D Biol. Crystallogr.* **50**, 760-763
58. Murshudov, G. N., Vagin, A. A., and Dodson, E. J. (1997) Refinement of macromolecular structures by the maximum-likelihood method. *Acta Crystallogr. D Biol. Crystallogr.* **53**, 240-255
59. Emsley, P., and Cowtan, K. (2004) Coot: model-building tools for molecular graphics. *Acta Crystallogr. D Biol. Crystallogr.* **60**, 2126-2132
60. Laskowski, R. A., MacArthur, M. W., Moss, D. S., and Thornton, J. M. (1993) PROCHECK: a program to check the stereochemical quality of protein structures. *J. Appl. Crystallogr.* **26**, 283-291
61. Kabsch, W. (1978) A discussion of the solution for the best rotation to relate two sets of vectors. *Acta Crystallogr. A* **34**, 827-828
62. Delano, W. L. (2002) *The PyMOL Molecular Graphics System*, DeLano Scientific LLC, San Carlos, CA.
63. Ochiai, A., Hashimoto, W., and Murata, K. (2006) A biosystem for alginate metabolism in *Agrobacterium tumefaciens* strain C58: molecular identification of Atu3025 as an exotype family PL-15 alginate lyase. *Res. Microbiol.* **157**, 642-649
64. Nedjma, M., Hoffmann, N., and Belarbi, A. (2001) Selective and sensitive detection of pectin lyase activity using a colorimetric test: application to the screening of microorganisms possessing pectin lyase activity. *Anal. Biochem.* **291**, 290-296
65. Edman, P. (1950) Method for determination of the amino acid sequence in peptides. *Acta Chem. Scand.* **4**, 7
66. Nishitani, Y., Maruyama, Y., Itoh, T., Mikami, B., Hashimoto, W., and Murata, K. (2012) Recognition of heteropolysaccharide alginate by periplasmic solute-binding proteins of a bacterial ABC transporter. *Biochemistry* **51**, 3622–3633
67. Hashimoto, W., Momma, K., Maruyama, Y., Yamasaki, M., Mikami, B., and Murata, K. (2005) Structure and function of bacterial super-biosystem responsible for import and depolymerization of macromolecules. *Biosci. Biotechnol. Biochem.* **69**, 673-692
68. Rossmann, M. G., Moras, D., and Olsen, K. W. (1974) Chemical and biological evolution of nucleotide-binding protein. *Nature* **250**, 194-199
69. Hoffmann, F., and Maser, E. (2007) Carbonyl reductases and pluripotent hydroxysteroid dehydrogenases of the short-chain dehydrogenase/reductase superfamily. *Drug Metab. Rev.* **39**, 87-144
70. Hashimoto, W., Kawai, S., and Murata, K. (2010) Bacterial supersystem for alginate import/metabolism and its environmental and bioenergy applications. *Bioeng. Bugs* **1**, 97-109

Acknowledgments- The authors thank Drs. S. Baba and N. Mizuno of the Japan Synchrotron Radiation Research Institute (JASRI) for their kind help in data collection. Diffraction data for crystals were collected at the BL-38B1 station of SPring-8 (Hyogo, Japan) with the approval (2011A1186, 2011B2055, 2012B1265, and 2013A1106) of JASRI. The authors also thank Drs. J. Ogawa and S. Kishino of the Division of Applied Life Sciences, Graduate School of Agriculture, Kyoto University for N-terminal sequence determination. The authors would also like to thank Dr. N. Takahashi of the Division of Applied Life Sciences, Graduate School of Agriculture, Kyoto University for analyzing the CD spectra.

Footnotes
This work was supported in part by grants-in-aid from the Japan Society for the Promotion of Science (to K. M. and W. H.), the Program for Promotion of Basic Research Activities for Innovative Biosciences (PROBRAIN) of Japan (to K.M.), the Targeted Proteins Research Program (to W. H.) from the Ministry of Education, Culture, Sports, Science, and Technology (MEXT) of Japan, and research fellowships from the Japan Society for the Promotion of Science for Young Scientists (to R. T.).

The nucleotide sequence of the A1-R′ gene (accession No. AB970509) has been deposited in the DDBJ/GenBank/EMBL databases. The atomic coordinates for the crystal structures of A1-R′ (code 4TKL), A1-R′/NAD^+ (code 4TKM), A1-R′_ex_W (code 4W7I), and A1-R_ex_W (code 4W7H) have been deposited in the Protein Data Bank (http://www.rcsb.org/).

The abbreviations used are as follows. WT: wild-type, DEH: 4-deoxy-L-*erythro*-5-hexoseulose uronate, KDG: 2-keto-3-deoxy-D-gluconate, SDR: short-chain dehydrogenase/reductase, PDB: Protein Data Bank, KPB: potassium phosphate buffer, CD: circular dichroism.

FIGURE LEGENDS

FIGURE 1. Alginate metabolic pathway in strain A1. Degradation and metabolism of alginate by strain A1 enzymes. Open and closed arrows indicate the cleavage sites of endo and exotype alginate lyases, respectively.

FIGURE 2. Construction scheme of plasmids for strain A1 mutant with a deficiency in A1-R. Black circle, plasmid; black bold arrow, A1-R gene; gray box, upstream and downstream 500 bp of the A1-R gene; shaded box, *Xho*I recognition site; open box, tetracycline resistance gene cassette.

FIGURE 3. Properties of A1-R′. (A) SDS-PAGE of purified A1-R′. Lane M, molecular weight standards; lane 1, purified nA1-R′ (5 μg); lane 2, purified rA1-R′ (5 μg). The arrow indicates the position of the enzyme. (B) Effects of pH and temperature on the activity and thermal stability of nA1-R′. Left: optimal pH. Activity was assayed with sodium acetate shown as diamond (♦) (pH 4.5, 5.5, 6.0, 6.5), KPB shown as square (■) (pH 5.4, 6.5, 6.9, 7.9), and glycine–NaOH shown as bullet (●) (pH 8.5, 9.1, 9.6, 10, 11). Sodium acetate appears to inhibit enzymatic activity compared with KPB. Activity at pH 6.5 in KPB was taken as 100%. Center: optimal temperature. Activity at 51°C was taken as 100%. Right: thermal stability. nA1-R′ was preincubated for 5 min at various temperatures (as indicated) and the residual enzymatic activity was measured. The activity of the enzyme preincubated at 4°C for 5 min was taken as 100%.

FIGURE 4. Sequence alignment. (A) Alignment between A1-R′ and A1-R. N-terminal determined residues of A1-R′ are underlined. (B) Alignment of NADH and NADPH-dependent SDR family enzymes. Conserved residues among SDR family enzymes, TGXXXGXG motif and catalytic triad (Ser, Tyr, and Lys) are indicated by open letters. Asterisk (*), colon (:), and period (.) indicate that residues are identical, highly similar, and moderately similar, respectively. Arrows and tubes over the alignment show β-strand and α-helix, respectively. Structural determinants (two loops) of the coenzyme requirement are boxed. Each enzyme is described as follows: D-3-HBDH, D-3-hydroxybutyrate dehydrogenase (PDB-ID, 2ZTL) from *Pseudomonas fragi*; 7α-HSDH, 7-α-hydroxysteroid dehydrogenase (PDB-ID, 1AHI) from *E. coli*; 15-HPDH, 15-hydroxy prostaglandin dehydrogenase (PDB-ID, 2DGZ) from *Homo sapiens*; β-keto-ACPR, β-keto-acyl carrier protein reductase (PDB-ID, 1EDO) from *Brassica napus*; ADH, alcohol dehydrogenase (PDB-ID, 1NXQ) from *Lactobacillus brevis*; SDH, serine dehydrogenase (PDB-ID, 3ASV) from *E. coli*.

FIGURE 5. Structures of A1-R′ and A1-R′/NAD^+. (A, B) Overall structure of A1-R′ superimposed on A1-R based on the main chain. Blue, A1-R′; gray, A1-R. The structure of B is rotated 90° toward the reader relative to that of A. (C, D) A1-R′/NAD^+ complex structure. A1-R′ molecule is shown as a ribbon model and each color indicates the following: blue, β-strand; red, α-helix, green: loop. NAD^+ molecule is shown by a stick model and each color indicates following: yellow, carbon atom; blue, nitrogen atom; orange, phosphorus atom; red, oxygen atom. The structure of D is rotated 90° toward the reader relative to that of C.

FIGURE 6. Comparison between A1-R′ and A1-R. (A) Coenzyme-binding site in A1-R′/NAD^+ complex structure. (B) Coenzyme-binding site in A1-R/$NADP^+$ complex structure (PDB-ID, 3AFN). Carbon atoms of NAD^+ or $NADP^+$ are colored pink. Residues within a distance of 4 Å from the coenzyme are shown. Blue, nitrogen atom; orange, phosphorus atom; red, oxygen atom. Carbon atoms of conserved and nonconserved residues between A1-R and A1-R′ are colored green and yellow, respectively. (C) Surface electrostatic potentials around NAD^+ molecule in A1-R′/NAD^+ complex structure. (D) Surface electrostatic potentials around $NADP^+$ molecule in A1-R/$NADP^+$ complex structure (PDB-ID, 3AFN). Electric charges are calculated at pH 7.0. Blue and red indicate basic and acidic, respectively. Green circle shows the binding site around the nucleoside ribose 2′ region of the coenzyme. (E) Relationship between loops and primary structure. A1-R′ is superimposed on A1-R based on the main chain. Loops and primary structure of A1-R′ and A1-R are colored red and yellow, respectively.

FIGURE 7. Structural validation of the WT and mutants of A1-R′ and A1-R. (A) CD profiles of WT A1-R′ and its mutants at 1 mg mL^{-1}. (B) CD profiles of WT A1-R and its mutants at 1 mg mL^{-1}. WT, ex_S, ex_L, and ex_W are colored blue, purple, red, and green, respectively, in panels A and B. (C) Superimposition of the main chains of A1-R′_ex_W (green) and WT A1-R′ (gray). (D) Superimposition of the main chains of A1-R_ex_W (blue) and WT A1-R (gray). (E) Fluorescence profiles of WT A1-R′ and its mutants used in the DSF analysis. (F) Fluorescence profiles of WT

A1-R and its mutants used in the DSF analysis. WT, ex_S, ex_L, and ex_W are colored blue, purple, red, and green, respectively, in panels E and F.

Table 1. Primers for cloning and site-directed mutagenesis.

Primer		Oligonucleotides
A1-R±500	forward	5′- CGCCGAGTACGAACAGTTCGCCCGGC -3′
	reverse	5′- CCACCAGCCGCTACGGTCGGTGTCATGC -3′
A1-R_G38D	sense	5′- CCAAGGTCGGCCTGCACGATCGCAAGGCACCCGCC -3′
	antisense	5′- GGCGGGTGCCTTGCGATCGTGCAGGCCGACCTTGG -3′
A1-R_XhoI	forward	5′- CTCGAGTTGCGCGGCGACGTCACTTACAAAC -3′
	reverse	5′- TCAGTGCTTGTACTGCCCGCCGTTGATGTCC -3′
A1-R′_NdeI		5′- AGGAGATATACATATGTTCAGCGATCTGAAGGGCAAGAGAATC -3′
A1-R′_BamHI		5′- GCTCGAATTCGGATCCTCAGGGGCAGATCTGGCCGCCG -3′
S150A	sense	5′- GTGATCAGTACGGGTGCGATCGCTGCGCGTGAA -3′
	antisense	5′- TTCACGCGCAGCGATCGCACCCGTACTGATCAC -3′
Y164F	sense	5′- GCGCGGGCGTCTTTGCGGCGTCCAA -3′
	antisense	5′- TTGGACGCCGCAAAGACGCCCGCGC -3′
K168A	sense	5′- CTATGCGGCGTCCGCGGCCTGGCTGCAC -3′
	antisense	5′- GTGCAGCCAGGCCGCGGACGCCGCATAG -3′
A1-R′_ex_S	forward	5′- CAGGGTATCGGGATGGCCACGGCCATTGAGC -3′
	reverse	5′- CGACGAGCCGGTGATGAGGATTCTCTTGCCCTTC -3′
A1-R′_ ex_L	forward	5′- CGCAAGGCACCGGCCGATCCGGCGTTGCTACTCGG -3′
	reverse	5′- GCCGTGGAGTCCGACCACGGCTCCATAGCGTGCCAG -3′
A1-R_ ex_S	forward	5′- GAGGGCATTGGCCTTGCCACCGCCCGC -3′
	reverse	5′- GGTCGAACCGGTGATCAGAACGCGCTTGCCTTTG -3′
A1-R_ ex_L	forward	5′- CACGTGGATCCCGCCAACATCGATGAGACCATCGCCAGC -3′
	reverse	5′- TGAATTCAGGCCGACCTTGGCGCCTGCACG -3′

Dotted, solid, and double underlines show identical sequence used in In-Fusion reaction, mutation site, and restriction site, respectively.

Table 2. Purification of native and recombinant A1-R′ enzymes.

	Total protein (mg)	Total activity (U)	Specific activity (U mg^{-1})	Yield (%)	Purification (fold)
Step		[NADH / NADPH]	[NADH / NADPH]	[NADH / NADPH]	[NADH / NADPH]
nA1-R′					
Cell extract	2050	3843 / 2065	1.87 / 1.01	100 / 100	1.00 / 1.00
TOYOPEARL DEAE-650M	330	1887 / 1322	5.72 / 4.01	49.1 / 64.0	3.05 / 3.97
TOYOPEARL Butyl-650M	32.7	1806 / 716.8	55.2 / 21.9	47.0 / 34.7	29.5 / 21.8
Superdex 200 pg	12.5	753.1 / 383.8	60.0 / 30.6	19.6 / 18.6	32.0 / 30.4
Hydroxylapatite	4.28	342.5 / 146.8	80.1 / 34.3	8.91 / 7.11	42.7 / 34.1
MonoQ HR	0.954	100.0 / 54.84	105 / 57.5	2.60 / 2.66	55.9 / 57.1
Superdex 75 pg	0.604	98.37 / 51.74	163 / 85.7	2.56 / 2.51	86.9 / 85.0
Q Sepharose HP	0.118	51.73 / 25.64	439 / 218	1.35 / 1.24	234 / 216
rA1-R′		[NADH]	[NADH]	[NADH]	[NADH]
Cell extract	1730	458000	265	100	1.00
TOYOPEARL DEAE-650M	945	263000	278	57.5	1.05
TOYOPEARL Butyl-650M	742	240000	323	52.4	1.22
Q Sepharose HP	313	129000	411	28.1	1.55
Superdex 200 pg	273	117000	428	25.5	1.62

Table 3. Effects of various compounds on the activity of nA1-R′

Compounds	Concentration (mM)	Activity (%)[a]
None (NADPH)		38[b]
(NADH)		100
Thiol reagents		
Dithiothreitol	1	97
Glutathione (reduced form)	1	107
2-Mercaptoethanol	1	107
Iodoacetic acid	1	98
p-Chloromercuribenzoic acid	1	94
Chelator		
EDTA	1	113
Sugars		
L-Fucose	5	98
D-Galactose	5	98
D-Glucose	5	100
D-Glucuronic acid	5	103
D-Mannose	5	102
L-Rhamnose	5	100
D-Xylose	5	98
D-Sucrose	5	101
D-Galacturonic acid	5	103
Metals		
$AlCl_3$	1	76
$MgCl_2$	1	115
$MnCl_2$	1	106
$CaCl_2$	1	121
$CoCl_2$	1	95
$ZnCl_2$	1	114
$HgCl_2$	0.01	83
NaCl	1	97
KCl	1	95
LiCl	1	102

[a] Relative activities (%) in a reaction mixture containing various compounds at the indicated concentrations are shown. The activity in the absence of the compound was taken as 100%.

[b] The value was determined when 0.2 mM NADH was replaced with 0.2 mM NADPH.

Table 4. Kinetic parameters of nA1-R′ and rA1-R for DEH, NADH, and NADPH.

	nA1-R′			rA1-R		
	k_{cat} (s^{-1})	K_m (μM)	k_{cat} K_m^{-1} (s^{-1} mM^{-1})	k_{cat} (s^{-1})	K_m (μM)	k_{cat} K_m^{-1} (s^{-1} mM^{-1})
DEH	227 ± 16.2	4790 ± 630	47.4	197 ± 8.9	1930 ± 98	102[(a)]
NADH	280 ± 10.2	15.5 ± 2.84	18100	25.3 ± 5.7	192 ± 75	132
NADPH	233 ± 44.6	224 ± 78	1040	220 ± 7.1	9.55 ± 1.4	23000

[a] The kinetic parameters of rA1-R for DEH are cited from (43)

Table 5. Statistics for X-ray diffraction and structure refinement.

	rA1-R′	rA1-R′ /NAD^+
Data collection		
Wavelength (Å)	1.0000	1.0000
Space group	$P3_121$	$P3_121$
Unit cell parameters (Å, °)	a = b = 87.7, c = 139.6	a = b = 87.9, c = 139.8
Resolution limit (Å)	50.0 – 1.80 (1.86-1.80)[a]	50.0 – 2.67 (2.77-2.67)[a]
Total reflections	682,105	219,436
Unique reflections	58,400	18,404
Redundancy	11.7 (11.4)	11.9 (12.2)
Completeness (%)	100 (100)	100 (99.9)
$I/\sigma(I)$	47.3 (5.8)	43.4 (9.0)
R_{merge} (%)	6.0 (38.4)	7.4 (30.6)
Wilson *B*-factor (Å^2)	17.4	38.3
Refinement		
Final model	483 residues, 306 water molecules	483 residues, 85 water molecules, 5 SO_4, 1 NAD^+
Resolution limit (Å)	33.4 – 1.80 (1.85 – 1.80)	33.5 – 2.67 (2.73 – 2.67)
Used reflections	55,375 (3,971)	17,397 (1,227)
Completeness (%)	99.8 (98.7)	99.7 (99.4)
R-factor (%)	18.2 (21.7)	19.4 (26.5)
R_{free} (%)	20.2 (24.5)	27.6 (35.5)
Average *B*-factor (Å^2)		
Protein		
Molecule A	23.5	47.5
Molecule B	24.8	52.2
Waters	33.6	38.5
PO_4		
Molecule C1	39.1	
Molecule C2	65.3	
Molecule C3	59.3	
NAD^+		61.3
SO_4		
Molecule E1		24.2
Molecule E2		62.0
Molecule E3		78.5
Molecule E4		63.8
Molecule E5		83.4
r.m.s.d.		
Bond (Å)	0.0046	0.0099
Angle (°)	0.97	1.40
Ramachandran plot (%)		
Favored regions	96.6	95.8
Allowed regions	3.0	3.8
Outliers	0.4	0.4

[a] Data on highest shells are given in parenthesis.

Table 6. Kinetic parameters of A1-R′ and A1-R mutants for NADH and NADPH.

Enzyme	NADH			NADPH			NADH/NADPH[a]	DEH		
	k_{cat} (s^{-1})	K_m (μM)	k_{cat} K_m^{-1} (s^{-1} mM^{-1})	k_{cat} (s^{-1})	K_m (μM)	k_{cat} K_m^{-1} (s^{-1} mM^{-1})		k_{cat} (s^{-1})	K_m (mM)	k_{cat} K_m^{-1} (s^{-1} mM^{-1})
A1-R′ Wild-type	274 ± 4.8	24.3 ± 1.5	11300	233 ± 15	272 ± 30	857	13	227 ±16.2	4.79 ± 0.63	47.4
A1-R′_ex_S	77.5 ± 4.7	20.4 ± 5.2	3800	109 ± 7.0	28.4 ± 6.9	3840	0.99	172 ± 2.65	3.32 ± 0.11	51.8
A1-R′_ex_L	33.6 ± 10	493 ± 220	68.2	110 ± 11	45.5 ± 15	2420	0.028	161 ± 6.31	2.77 ± 0.24	58.1
A1-R′_ex_W	134 ± 26	217 ± 78	618	149 ± 1.3	2.85 ± 0.31	52300	0.012	225 ± 6.65	4.45 ± 0.25	50.6
A1-R Wild-type	25.3 ± 5.7	192 ± 75	132	220 ± 7.1	9.55 ± 1.4	23000	0.0057	197 ± 8.9	1.93 ± 0.098	102
A1-R_ex_S	3.77 ± 0.47	623 ± 100	6.05	193 ± 18	512 ± 70	377	0.016	226 ± 6.02	3.54 ± 0.19	48.9
A1-R_ex_L	4.25 ± 2.0	321 ± 240	13.2	N.D.	N.D.	N.D.	N.D.	5.47 ± 0.186	1.66 ± 0.15	1.32
A1-R_ex_W	6.80 ± 3.5	2580 ± 1400	2.64	2.03 ± 3.0	5600 ± 8600	0.363	7.27	8.66 ± 0.257	3.04 ± 0.19	2.85

N.D.: not determined due to low activity.

[a] The k_{cat} K_m^{-1} value toward NADH/ the k_{cat} K_m^{-1} value toward NADPH.

Figure 1.

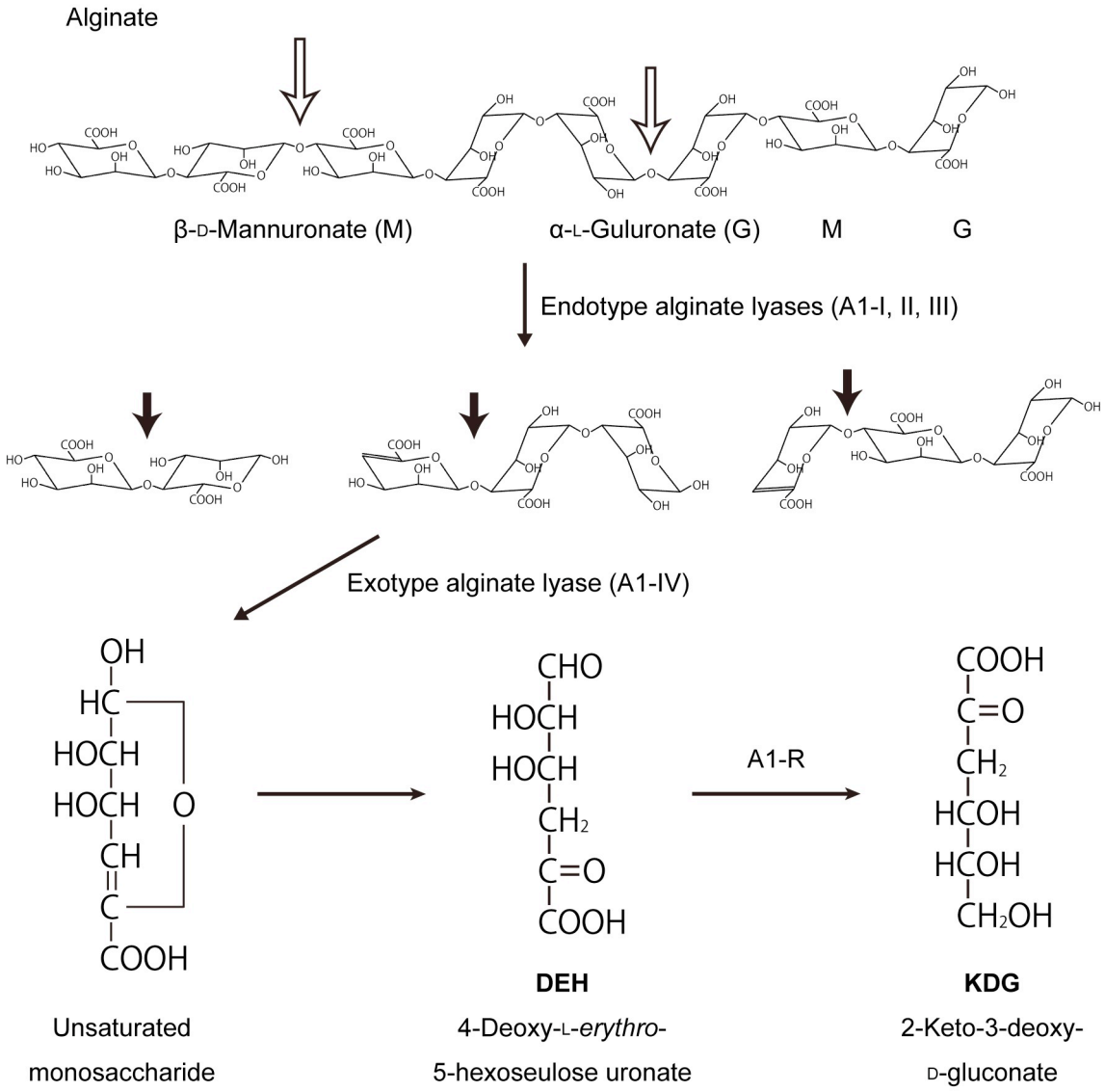
Alginate
β-D-Mannuronate (M)
α-L-Guluronate (G)
M
G
Endotype alginate lyases (A1-I, II, III)
Exotype alginate lyase (A1-IV)
A1-R
Unsaturated monosaccharide
DEH
4-Deoxy-L-erythro-5-hexoseulose uronate
KDG
2-Keto-3-deoxy-D-gluconate

Figure 2.

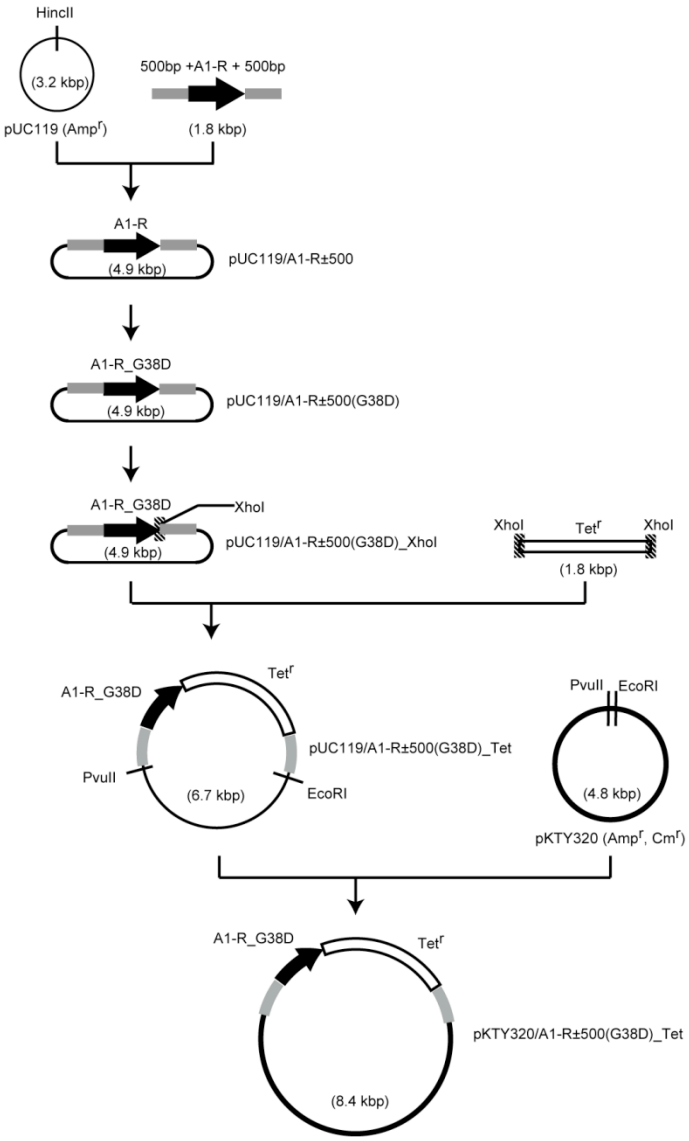
HincII
(3.2 kbp)
pUC119 (Amp^r)
500bp +A1-R + 500bp
(1.8 kbp)
A1-R
(4.9 kbp)
pUC119/A1-R±500
A1-R_G38D
(4.9 kbp)
pUC119/A1-R±500(G38D)
A1-R_G38D
XhoI
(4.9 kbp)
pUC119/A1-R±500(G38D)_XhoI
XhoI
Tet^r
XhoI
(1.8 kbp)
A1-R_G38D
Tet^r
PvuII
EcoRI
(6.7 kbp)
pUC119/A1-R±500(G38D)_Tet
PvuII
EcoRI
(4.8 kbp)
pKTY320 (Amp^r, Cm^r)
A1-R_G38D
Tet^r
(8.4 kbp)
pKTY320/A1-R±500(G38D)_Tet

Figure 3.

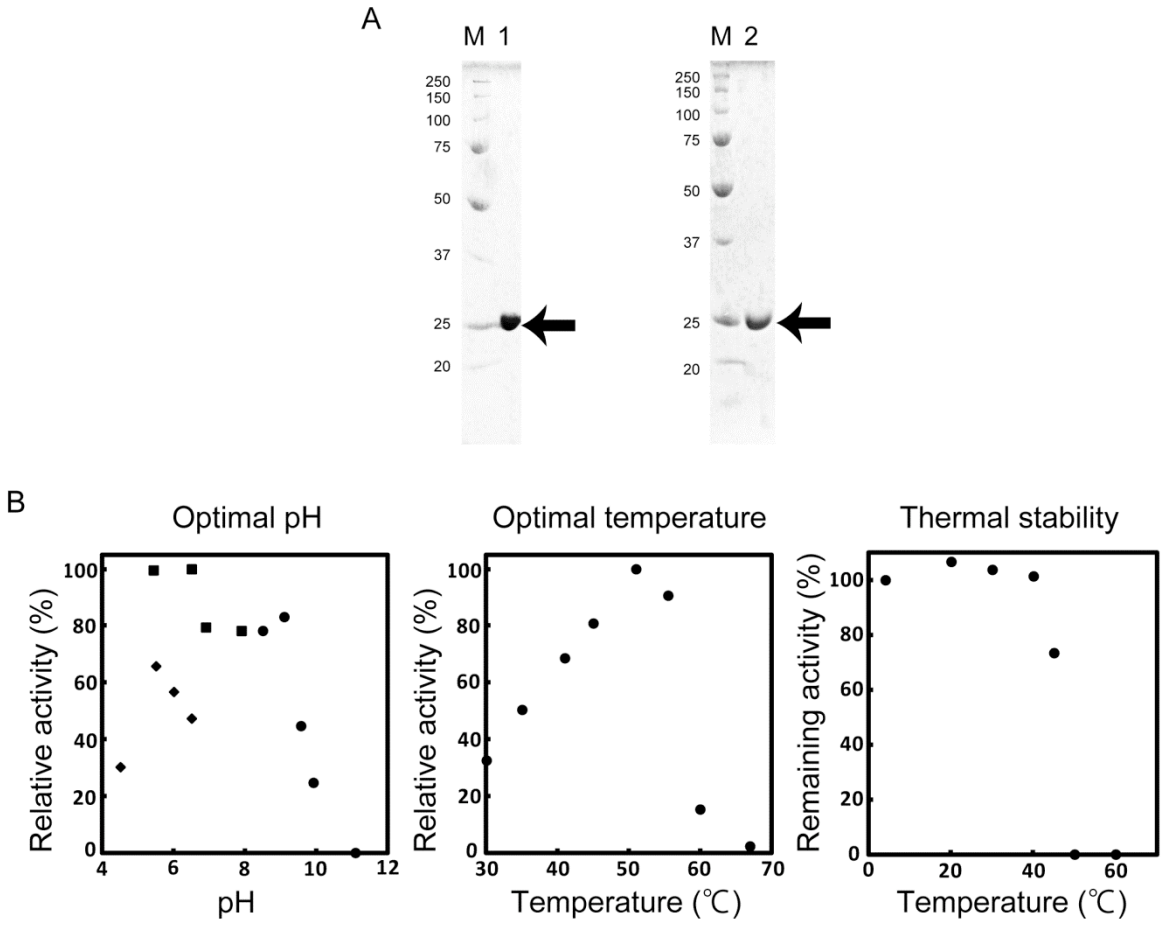
A
M 1
M 2
250
150
100
75
50
37
25
20
B
Optimal pH
Relative activity (%)
pH
Optimal temperature
Relative activity (%)
Temperature (℃)
Thermal stability
Remaining activity (%)
Temperature (℃)

Figure 4.

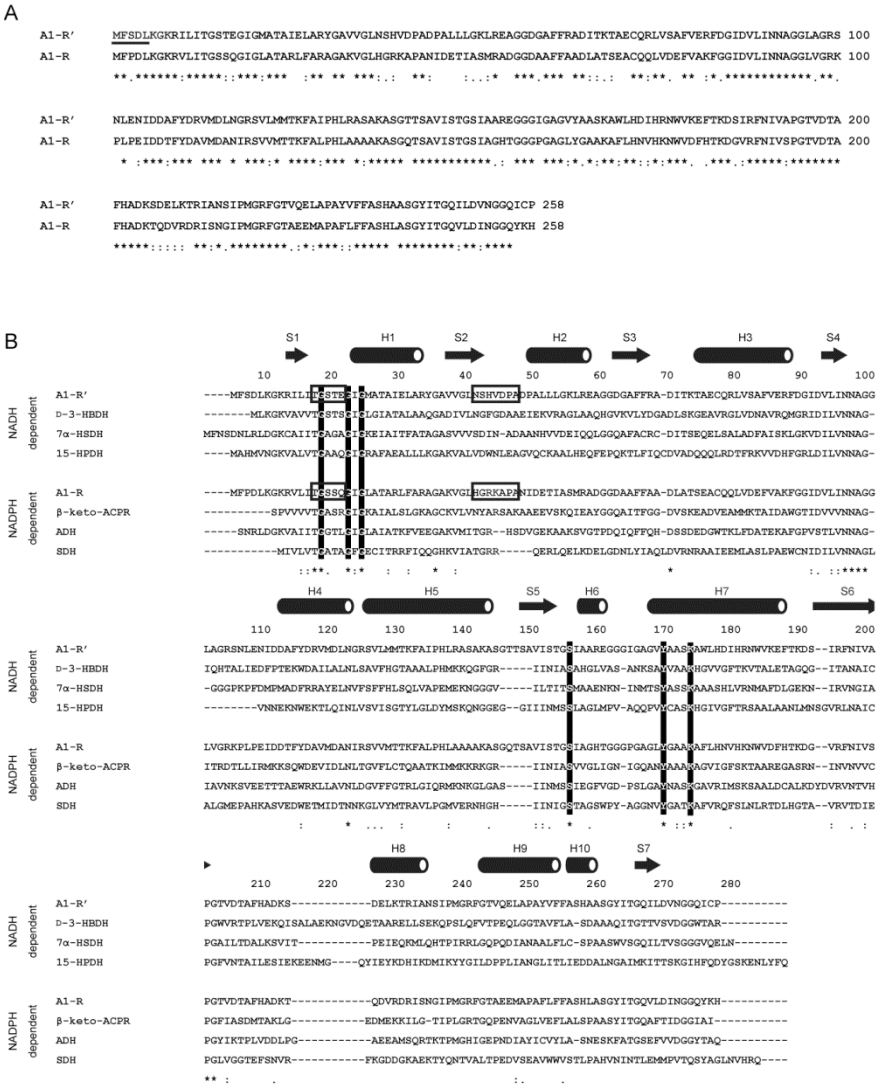
A
A1-R′ MFSDLKGKRILITGSTEGIGMATAIELARYGAVVGLNSHVDPADPALLLGKLREAGGDGAFFRADITKTAECQRLVSAFVERFDGIDVLINNAGGLAGRS 100
A1-R MFPDLKGKRVLITGSSQGIGLATARLFARAGAKVGLHGRKAPANIDETIASMRADGGDAAFFAADLATSEACQQLVDEFVAKFGGIDVLINNAGGLVGRK 100
A1-R′ NLENIDDAFYDRVMDLNGRSVLMMTKFAIPHLRASAKASGTTSAVISTGSIAAREGGGIGAGVYAASKAWLHDIHRNWVKEFTKDSIRFNIVAPGTVDTA 200
A1-R PLPEIDDTFYDAVMDANIRSVVMTTKFALPHLAAAAKASGQTSAVISTGSIAGHTGGGPGAGLYGAAKAFLHNVHKNWVDFHTKDGVRFNIVSPGTVDTA 200
A1-R′ FHADKSDELKTRIANSIPMGRFGTVQELAPAYVFFASHAASGYITGQILDVNGGQICP 258
A1-R FHADKTQDVRDRISNGIPMGRFGTAEEMAPAFLFFASHLASGYITGQVLDINGGQYKH 258
B
S1 H1 S2 H2 S3 H3 S4
H4 H5 S5 H6 H7 S6
H8 H9 H10 S7
NADH dependent
NADPH dependent
A1-R′
D-3-HBDH
7α-HSDH
15-HPDH
A1-R
β-keto-ACPR
ADH
SDH

Figure 5.

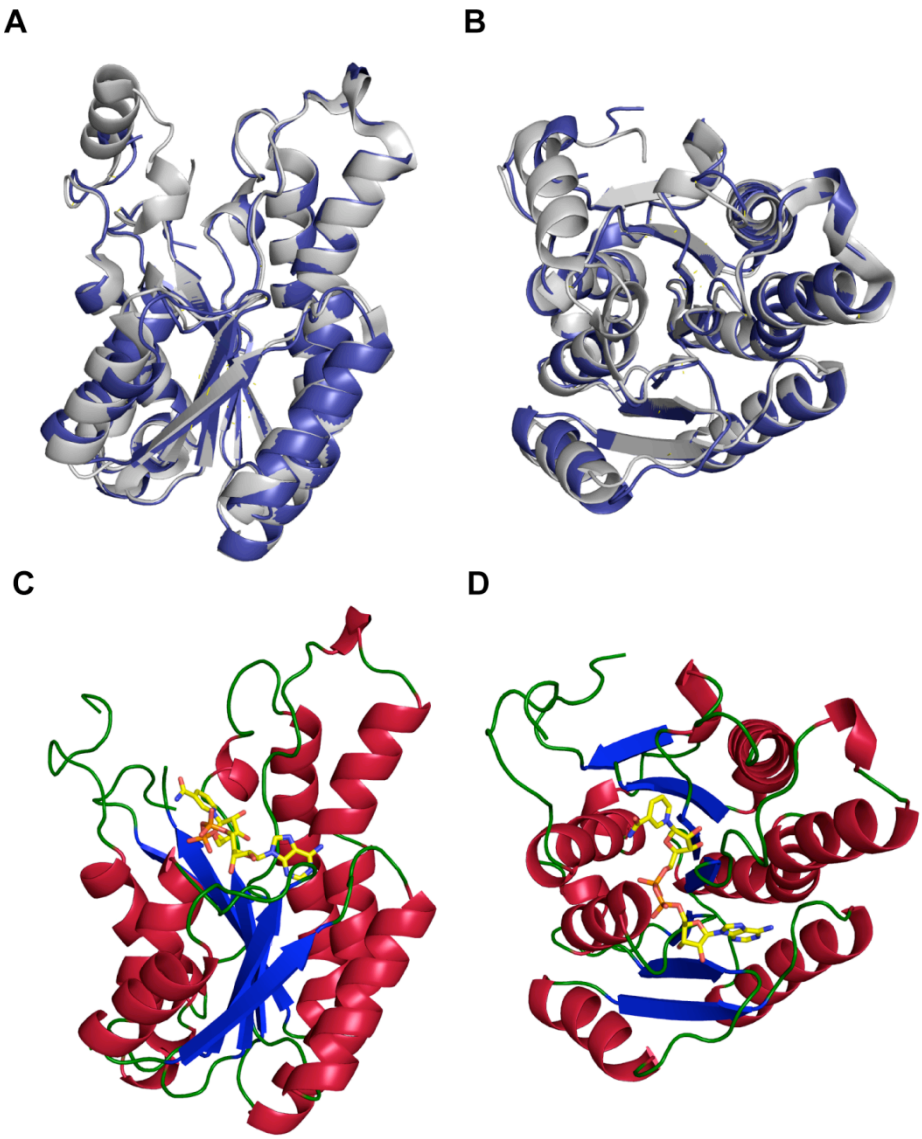

Figure 6.

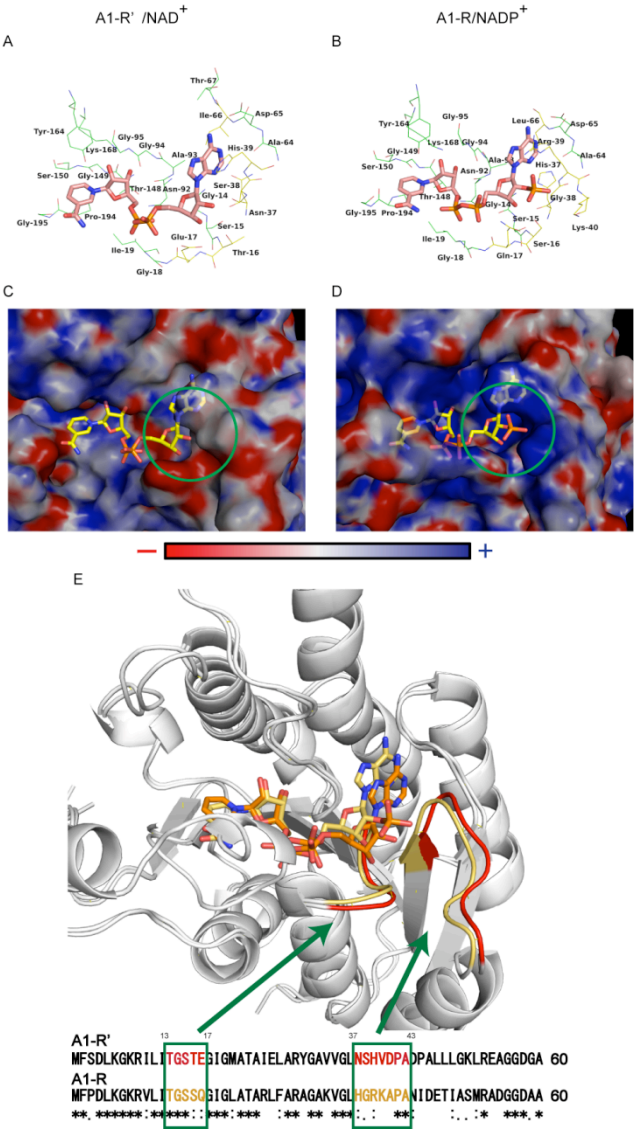
A1-R' /NAD+
A1-R/NADP+
A
B
C
D
E
A1-R'
MFSDLKGKRILITGSTEGIGMATAIELARYGAVVGLNSHVDPADPALLGKLREAGGDGA 60
A1-R
MFPDLKGKRVLITGSSQGIGLATARLFARAGAKVGLHGRKAPANIDETIASMRADGGDAA 60

Figure 7.

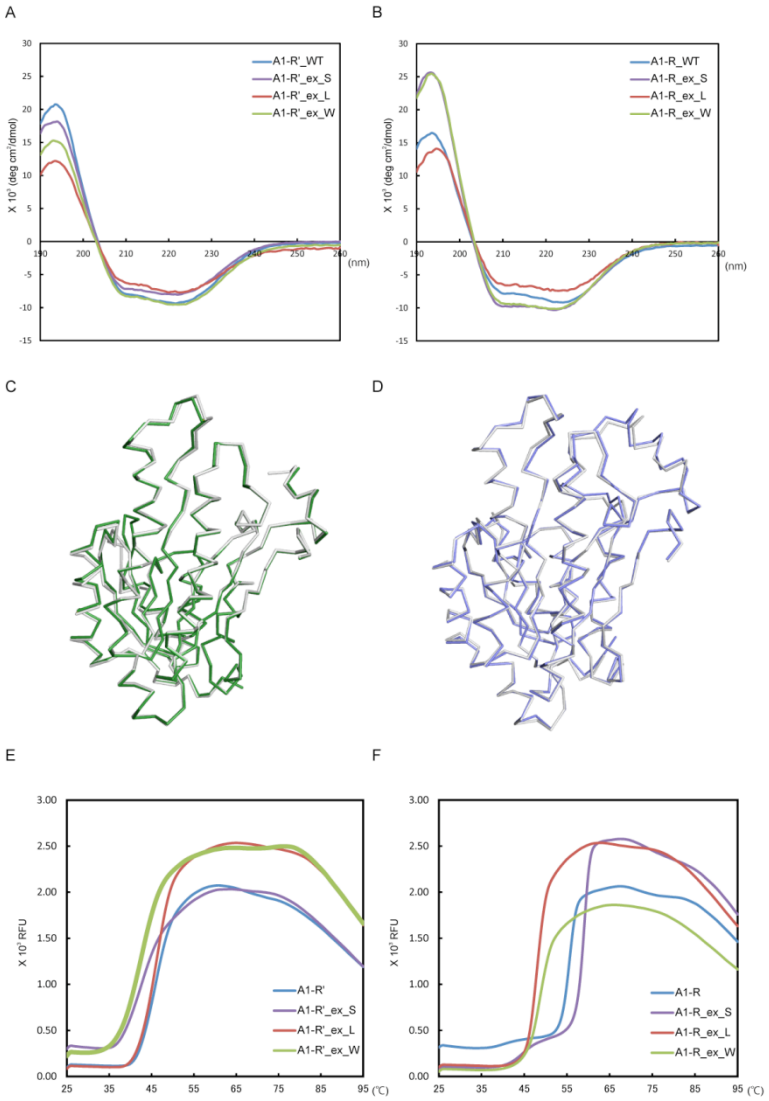
A
B
A1-R'_WT
A1-R'_ex_S
A1-R'_ex_L
A1-R'_ex_W
A1-R_WT
A1-R_ex_S
A1-R_ex_L
A1-R_ex_W
X 10³ (deg cm²/dmol)
(nm)
C
D
E
F
X 10³ RFU
A1-R'
A1-R'_ex_S
A1-R'_ex_L
A1-R'_ex_W
A1-R
A1-R_ex_S
A1-R_ex_L
A1-R_ex_W
(℃)